Sensors and Materials, Vol. 27, No. 1 (2015) 35–42
MYU Tokyo

S & M 1043

15 mA Bidirectional Laser Triggering in Two-Terminal Microdevices Based on Vanadium Dioxide Thin Films

Eung-Soo Kim, Songhyun Jo[1], Kyongsoo Park[1], Young-Suk Kim[1] and Yong Wook Lee[1,2,*]

Division of Digital Media Engineering, Busan University of Foreign Studies, 65 Geumsaem-ro 485 beon-gil, Geumjeong-gu, Busan 609-815, Korea
[1]Interdisciplinary Program of Biomedical Mechanical & Electrical Engineering, Pukyong National University, 45 Yongso-ro, Nam-gu, Busan 608-737, Korea
[2]School of Electrical Engineering, Pukyong National University, 45 Yongso-ro, Nam-gu, Busan 608-737, Korea

(Received July 14, 2014; accepted December 8, 2014)

Key words: vanadium dioxide, thin film, phase transition, microdevice, photoexcitation

By using an infrared laser diode with an oscillating wavelength of 1550 nm, we demonstrated 15 mA bidirectional laser triggering with an amplitude switching ratio of ~78.9 in a two-terminal microdevice based on a vanadium dioxide (VO_2) thin film, which was DC-biased at 3.35 V. The VO_2-based device has only one conducting layer, i.e., one VO_2 patch, which facilitates the use of the triggering laser with a reduced spot diameter. The reduced beam spot can increase the maximum on-state current at the same illumination power, resulting in the improvement of the amplitude switching ratio. A specific bias voltage range enabling the bidirectional laser triggering was experimentally determined from the current-voltage characteristics of the VO_2-based device with an electrode separation of 10 μm and a current channel width of 30 μm, which was measured in a current-controlled mode. In a closed-loop circuit constructed by serially connecting a standard resistor, a DC voltage source, and the device, the transient responses of light-triggered currents were also observed for response time analysis.

1. Introduction

Vanadium dioxide (VO_2) is a representative strongly correlated material showing an insulator-to-metal or metal-to-insulator phase transition (PT) induced by external stimuli such as temperature,[(1)] pressure,[(2)] and light.[(3)] This PT property of VO_2 causes highly nonlinear current–voltage (I–V) behavior in two-terminal devices based on VO_2

*Corresponding author: e-mail: yongwook@pknu.ac.kr

thin films, resulting in abrupt jumps of electrical currents.[4] The threshold voltage of the device, after which a current jump occurs triggering the PT of VO_2, is changed by illuminating the VO_2 film with an infrared laser,[5,6] and this laser-assisted switching is a basic function for the application of VO_2-based devices to laser-triggered switches. In previous works, the maximum on-state current of the laser-triggered VO_2 device was ~3.9 mA with an amplitude ratio of less than 4 between switched variables (on- and off-state currents).[5] Recently, 10 mA bidirectional laser triggering has been realized with an amplitude switching ratio of ~68.2 by incorporating VO_2 devices with parallel conducting layers.[7] For VO_2-based devices to be considered for the practical application of optically gated switches such as light-triggered thyristors, numerous device parameters including the maximum on-state current, the amplitude switching ratio, and the off-state current should be significantly improved. In the optical triggering of VO_2 devices, efforts for the enhancement of these parameters have been relatively insufficient, and most studies focused on the modulation of the optical properties of VO_2 thin films, such as the refractive index and the transmittance.[8–13] Some works on electrical switching devices based on VO_2 thin films were reported by utilizing electrical pulses applied to two-terminal VO_2-based devices.[14,15]

In this study, we demonstrated 15 mA bidirectional laser triggering in a two-terminal microdevice based on a VO_2 thin film, fabricated by a sol-gel method, by using an approximately 1550 nm infrared laser diode (LD). The bidirectional laser triggering indicates that the forward or reverse PT of VO_2 is triggered in accordance with the switched state (on- or off-state) of the LD. The bidirectional laser triggering can be regarded as optically controlled threshold switching realized by photoassisted negative differential resistance (NDR) reduction of VO_2.[7,16] Here, unlike the devices used in the previous study,[7] the VO_2 device has only one conducting layer, i.e., one VO_2 patch, which facilitates the use of an illumination laser with a reduced beam diameter. The reduced beam spot can increase the maximum on-state current at the same illumination power, resulting in the improvement of the amplitude switching ratio. In the following section, the experimental setup for inducing the laser triggering in the VO_2 device will be explained including the fabrication of the device and the closed-loop circuit for measuring the transient response of laser-triggered current. The *I–V* characteristics of the device triggered by the LD will be analyzed. Then, the transient response of the laser-triggered device will be investigated.

2. Experimental Preparation

Figure 1(a) shows the experimental setup for 15 mA laser triggering in a two-terminal VO_2-based microdevice. An inset of Fig. 1(a) shows the plane-view optical microscopy image of the fabricated device (L = 10 μm and W = 30 μm). The cross-sectional-view schematic diagram of the fabricated device is shown on the lower left side of Fig. 1(a). VO_2 thin films whose average thickness was ~100 nm were grown on sapphire (Al_2O_3) substrates by sol-gel deposition.[17] The sol-gel deposition method is composed of a series of spin coating and subsequent annealing processes. The 0.12 M solution for the spin coating process was prepared by synthesizing vanadium triisopropoxide,

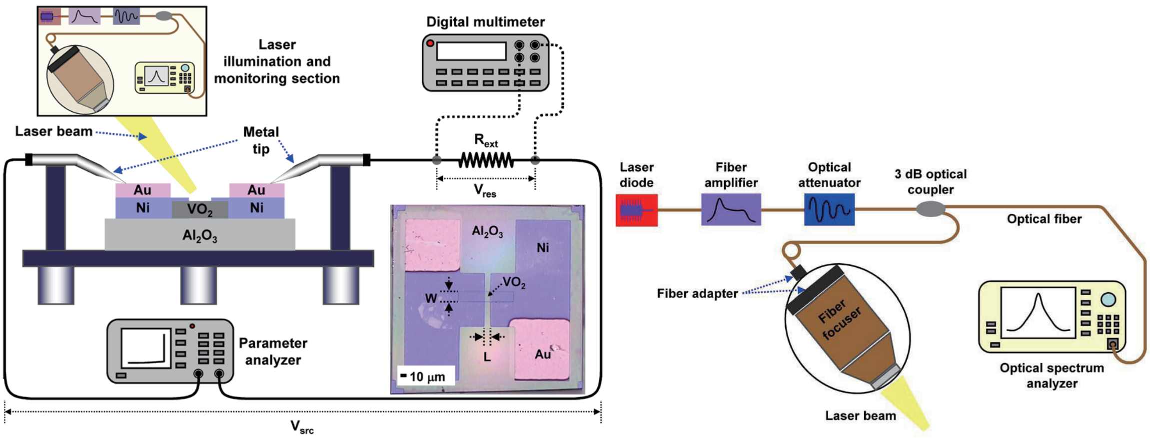

(a) (b)

Fig. 1. (Color online) (a) Experimental setup for 15 mA laser triggering in VO_2-based device and (b) laser illumination and monitoring section. An inset of (a) shows the optical microscopy image of the fabricated device.

$VO(OC_3H_7)_3$ (Stream Ltd., USA), in isopropanol using acetic acid as a catalyst. The prepared solution was spin-coated onto Al_2O_3 substrates at a spin rate of 2000 rpm for 20 s. Then, in order to remove the excess alcohol, the coated film was baked on a hot plate at 250 °C for 3 min. All the processes were performed in air to partially hydrolyze the alkoxide film with ambient moisture and repeated three times in a row. The final annealing process was carried out at 410 °C for 30 min in air. To form the VO_2 phase through a reduction process, additional annealing of the film was carried out at a low oxygen pressure. By utilizing a photolithographic technique, Au/Ni electrodes were formed on etched VO_2 films to fabricate two-terminal microdevices. *L* and *W* indicate the electrode separation and the width of the VO_2 patch, respectively. In the laser illumination and monitoring section shown in Fig. 1(b), the output of a distributed feedback LD (Thorlabs S3FC1550) was amplified by an optical fiber amplifier (Luxpert LXI-2000). The typical output power and side-mode suppression ratio of the LD were ~1.5 mW and > 40 dB, respectively, and its output power stability was ±0.1 dB for 24 h. The amplified optical power was adjusted by an optical attenuator with a dynamic range of 60 dB. The attenuator output was separated into two light components via a 3 dB optical coupler.[18] One component was introduced into a fiber-pigtailed focuser to focus an incident beam on the VO_2 film, and the other component into an optical spectrum analyzer (Yokogawa AQ6370) for spectral monitoring. The beam emerging from the focuser illuminated the film at 30° incidence. The spot diameter and working distance of the focuser were ~18 μm and ~10 mm, respectively, and its position was set using an *xyz* translation stage for the surface spot diameter to be ~90 μm. The optical density of the beam was ~157.2 W/cm² at an input power of 10 mW. For measuring the *I–V* property of the device, a parameter analyzer (HP 4156C) and a microprobe station were utilized. Transient responses of electrical currents were measured in a closed-loop circuit, shown in Fig. 1(a), constructed by serially connecting a resistor with the resistance R_{ext}, the parameter analyzer as a voltage source for the DC bias V_{src}, and the device, by monitoring the voltage across R_{ext} using a digital multimeter (Keithley 2000).

3. Experimental Results and Discussion

Figure 2(a) shows the photoinduced *I–V* characteristics of the fabricated VO_2-based device (L = 10 μm and W = 10 μm), measured in a current-controlled or I-mode. The optical power of the illumination laser with a wavelength of ~1549.99 nm was varied from −40 to 11 dBm, and the current compliance was set as 2 mA. As can be seen from the figure, upper and lower threshold voltages ($V_{th1,off}$ and $V_{th2,off}$) decrease with increasing illumination power. For example, $V_{th1,off}$ decreases from ~9.6 to ~4.1 V at an illumination power of 11 dBm. In particular, the difference between the two threshold voltages ($V_{th1,off}$ and $V_{th2,off}$) also decreases, resulting in the collapse of the NDR region as the illumination power increases. The fabricated devices showed good repeatability in *I–V* measurements for continuous wave laser illumination (~1550 nm) up to ~1500 W/cm².

Figure 2(b) shows the *I–V* characteristics of the fabricated device (L = 10 μm and W = 30 μm), measured in the I-mode with the laser switched off or on, indicated as blue squares or red circles, respectively. The current compliance was set as 15 mA, which corresponded to 500 kA/cm² in the device. The optical power, wavelength, and signal-to-noise ratio of the illumination laser were ~11.60 dBm, ~1549.99 nm, and ~56.69 dB, respectively. When the laser was switched off, the upper and lower threshold voltages,

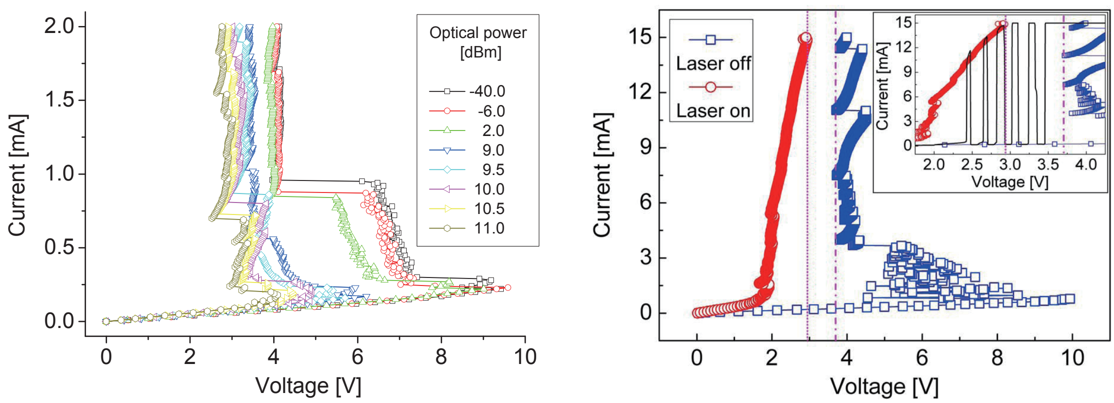

(a) (b)

Fig. 2. (Color online) (a) Photoinduced *I–V* characteristics of fabricated device (L = 10 μm and W = 10 μm) measured in I-mode and (b) *I–V* characteristics of fabricated device (L = 10 μm and W = 30 μm) measured in I-mode with laser switched off (blue squares) or on (red circles).

$V_{th1,off}$ and $V_{th2,off}$, of the device were measured as ~9.94 and ~3.71 V, respectively. Because the LD emits a Gaussian beam, the tolerance limit with respect to the spatial deviation of the beam spot is wider in the transverse direction of VO_2 patches than in the longitudinal direction. In the laser excitation of VO_2, the portion of VO_2 metallic grains increases with the illumination power, resulting in the decrease in threshold voltage.(19) Therefore, if the position and power of the aligned beam are fixed, it is expected that there will be no significant difference in threshold voltage, although the beam profile will change from a Gaussian distribution to a uniform distribution.(7)

With the laser switched on, NDR seems to almost disappear, suppressing threshold switching. Although the upper threshold voltage ($V_{th1,on}$) is not definitely determined, the lower threshold voltage ($V_{th2,on}$) can be determined to be ~1.66 V. The voltage at the compliance current (~2.94 V), indicated as a dotted line, can act as the effective upper threshold voltage ($V_{th1,eff,on}$) in the laser triggering operation. Bidirectional laser triggering can be achieved in a specific V_{src} range between $V_{th1,eff,on}$ and $V_{th2,off}$ (~2.94 and ~3.71 V), i.e., a voltage region between dotted and dash-dotted lines. We will designate this specific V_{src} region as Region S for convenience. On the other hand, unidirectional laser triggering, in which the reverse PT of VO_2 does not occur even when switching the laser off, occurs at $V_{src} > V_{th2,off}$. Thus, V_{src} was selected as 3.35 V to induce bidirectional laser triggering.

This can be confirmed from the inset of Fig. 2(b), which shows optically controlled switching characteristics of the VO_2 device under V_{src} increase from 0 to 4 V with the laser randomly switched on or off six times per state. In the V_{src} range of 2.0–3.4 V, the first five bidirectional triggering operations are obtained, and at V_{src} > 3.4 V, the device current that jumps to 15 mA with the turning on of the laser does not fall after the turning off of the laser, that is, unidirectional triggering operation is observed at the sixth triggering operation. It can be inferred from this optical gating (triggering) result that the bidirectional triggering regime and, in particular, the maximum on-state current of the optically triggered device are directly determined by the *I–V* behavior of the device, measured in the I-mode with the laser switched on or off. In addition, it is found that an effective bidirectional triggering region is smaller than Region S owing to the laser heating effect. For example, because the *I–V* curves in Fig. 2(b) are measured at ~3 s after switching the continuous wave laser on or off, the $V_{th2,off}$ of the device that experiences the instantaneous change in illumination power is slightly smaller than the upper limit (~3.71 V) of Region S.

Figure 3 shows the transient responses of laser-triggered devices for various on-state temporal durations. The compliance current was also set as 15 mA for all transient responses. Figures 3(a) and 3(b) show the transient responses of the fabricated VO_2 device laser-triggered for relatively shorter (5, 10, and 20 s) and longer (30, 60, and 120 s) on-state durations, respectively, in the closed-loop circuit with R_{ext} = 10 Ω and V_{src} = 3.35 V. In Fig. 3(a), the bidirectional triggering operation was performed five times for each on-state duration. The off-state duration, i.e., the illumination-free interval between two adjacent triggering operations, was set to be the same as the corresponding on-state duration, except for the interval between two triggering operations with different on-state durations. In Fig. 3(b), six bidirectional triggering operations were sequentially

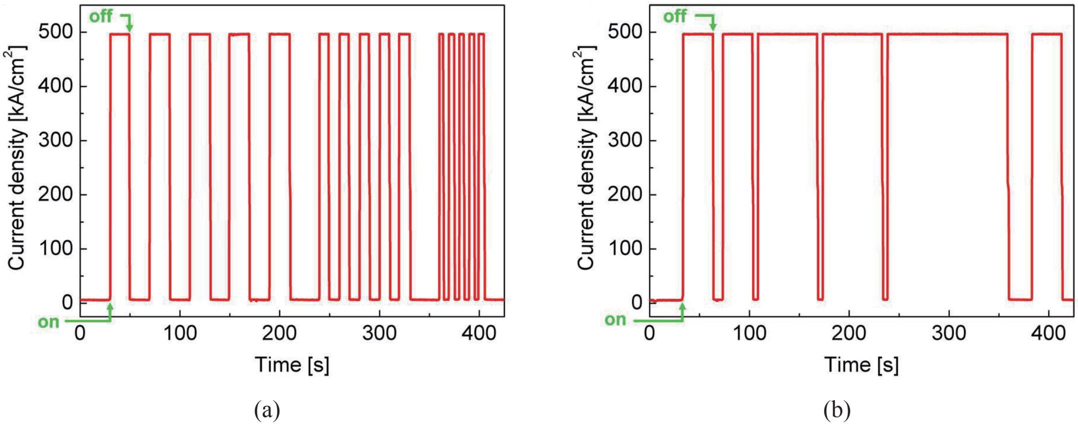

Fig. 3. (Color online) Transient responses of laser-triggered device for relatively (a) short on-state durations (5, 10, and 20 s) and (b) long on-state durations (30, 60, and 120 s). In the closed loop circuit, the VO_2 device was biased at V_{src} = 3.35 V with R_{ext} = 10 Ω.

performed for on-state durations of 30, 30, 60, 60, 120, and 30 s, and off-state durations, unlike the case in Fig. 3(a), were irregularly selected among 5, 10, and 20 s. It was observed from the measured responses that stable bidirectional switching between ~0.19 and 15 mA can be obtained at V_{src} = 3.35 V for various on- or off-state durations. The average amplitude switching ratio was evaluated as ~78.9 in the bidirectional laser triggering of the fabricated device.

In particular, the rising time was measured as ~192 ms regardless of the on-state duration, which was similar to the minimum data acquisition time step in our experimental setup. The actual rising time is expected to be shorter than the measured one, and the measured response time will decrease if data acquisition is performed at a higher rate. The rising time can also be affected by the long switching time of the laser driving current pulse. The falling time, measured as ~608 ms, was longer than the rising time, but it also showed little dependence on the on-state duration. Slower falling was attributed to the laser heating effect and increased thermal conductivity in the metallic state of VO_2. In the laser-induced PT, the thermally induced PT dominates over photoexcitation at an illumination power higher than 30 mW.(19) Laser-induced heating increases the portion of metallic VO_2 grains in the VO_2 film and decreases the threshold voltage of the VO_2 device while reducing a bidirectional triggering region such as Region S. The reduction of the bidirectional triggering region deteriorates the amplitude switching ratio owing to the increase in off-state current. Here, we focused on the on-state durations, which are on the order of 10 s, to examine the laser-induced heating effect, coupled with the photoinduced PT. Previous studies related to the thermal switching of VO_2 reported a switching time of 1–3 ms,(8,9) and the voltage-triggered PT has an ultrashort switching time of ~2 ns.(15) If another data collection instrument with a high sampling rate is used for shorter on-state durations, it is expected for the actual switching time to be on the order of ms. In particular, the response time can be further improved by incorporating high-speed external optical switches to generate short laser pulses or thermoelectric coolers to control the device temperature affected by laser-induced heating. Moreover, the thickness dependence of the device performance should be considered. Generally, the average VO_2 grain size increases with the increase in the thickness of the VO_2 film. The amplitude and sharpness of the thermal PT of VO_2 are directly correlated with the grain size. With the increase in grain size, resulting from the increase in film thickness, the density of grain boundaries and associated defects decreases, causing a stronger and sharper transition. On the other hand, the amplitude of hysteresis curves decreases with the decrease in film thickness.[19] This will lead to the decrease in maximum on-state current and thus amplitude switching ratio.

4. Conclusions

We demonstrated bidirectional laser triggering in a two-terminal planar VO_2 device using an approximately 1550 nm LD. A maximum on-state current of 15 mA and an amplitude switching ratio of ~78.9 were attained in the VO_2 device DC-biased at 3.35 V, and the transient response of light-triggered currents was also analyzed. The high amplitude switching ratio coupled with the bidirectional switching capability could lead to further interest in the use of light-triggered oxide devices for future electronic power devices and sensing systems.[20]

Acknowledgements

This research was supported by the Korea Electric Power Corporation Research Institute through the Korea Electrical Engineering & Science Research Institute (grant number: R13TA12).

References

1 F. J. Morin: Phys. Rev. Lett. **3** (1959) 34.
2 E. Arcangeletti, L. Baldassarre, D. D. Castro, S. Lupi, L. Malavasi, C. Marini, A. Perucchi and P. Postorino: Phys. Rev. Lett. **98** (2007) 196406.
3 A. Cavalleri, Cs. Tóth, C. W. Siders, J. A. Squier, F. Ráksi, P. Forget and J. C. Kieffer: Phys. Rev. Lett. **87** (2001) 237401.
4 Y. W. Lee, B.-J. Kim, J.-W. Lim, S. J. Yun, S. Choi, B.-G. Chae, G. Kim and H.-T. Kim: Appl. Phys. Lett. **92** (2008) 162903.
5 Y. W. Lee, B.-J. Kim, S. Choi, H.-T. Kim and G. Kim: Opt. Express **15** (2007) 12108.
6 Y. W. Lee, E.-S. Kim, B.-S. Shin and S.-M. Lee: KIEE J. Electr. Eng. Technol. **7** (2012) 784.
7 B.-J. Kim, G. Seo and Y. W. Lee: Opt. Express **22** (2014) 9016.
8 S. Chen, H. Ma, X. Yi, H. Wang, X. Tao, M. Chen, X. Li and C. Ke: Infrared Phys. Technol. **45** (2004) 239.
9 H. Wang, X. Yi, S. Chen and X. Fua: Sens. Actuators, A **122** (2005) 108.
10 R. M. Briggs, I. M. Pryce and H. A. Atwater: Opt. Express **18** (2010) 11192.
11 J. D. Ryckman, V. Diez-Blanco, J. Nag, R. E. Marvel, B. K. Choi, R. F. Haglund and S. M. Weiss: Opt. Express **20** (2012) 13215.

12 J. D. Ryckman, K. A. Hallman, R. E. Marvel, R. F. Haglund and S. M. Weiss: Opt. Express **21** (2013) 10753.
13 P. A. Do, A. Hendaoui, E. Mortazy, M. Chaker and A. Hache: Opt. Commun. **288** (2013) 23.
14 B.-G. Chae, H.-T. Kim, D.-H. Youn and K.-Y. Kang: Physica B **369** (2005) 76.
15 Y. Zhou, X. Chen, C. Ko, Z. Yang, C. Mouli and S. Ramanathan: IEEE Electron Dev. Lett. **34** (2013) 220.
16 N.-S. Lee, J.-S. Chang, and Y.-S. Kwon: KIEE J. Electr. Eng. Technol. **1** (2006) 366.
17 B.-G. Chae, H.-T. Kim, S. J. Yun, Y. W. Lee, B.-J. Kim, D.-H. Youn and K.-Y. Kang: Electrochem. Solid-State Lett. **9** (2006) C12.
18 Y.-K Choi: KIEE J. Electr. Eng. Technol. **4** (2009) 287.
19 G. Seo, B.-J. Kim, H.-T. Kim and Y. W. Lee: J. Lightwave Technol. **30** (2012) 2718.
20 B. V. Manikandan, S. C. Raja and P. Venkatesh: KIEE J. Electr. Eng. Technol. **6** (2011) 14.